metals

Article

The Influence of Different External Fields on Aging Kinetics of 2219 Aluminum Alloy

Lihua Zhan [1,2,*], Wenke Li [1], Qiangqiang Ma [1] and Lingfeng Liu [1]

1 Light Metal Research Institute, Central South University, Changsha 410083, China; lwk1992@csu.edu.cn (W.L.); wuhu112@yeah.net (Q.M.); goodlucky321@yeah.net (L.L.)
2 National Key Laboratory of High Performance Complex Manufacturing, Central South University, Changsha 410083, China
* Correspondence: yjs-cast@csu.edu.cn; Tel.: +86-371-88830254

Academic Editor: Hugo F. Lopez
Received: 19 July 2016; Accepted: 15 August 2016; Published: 26 August 2016

Abstract: By undertakig an aging experiment on 2219 aluminum alloy under different external field and by the method of hardness test, a comparative study on the kinetics of aging generated under different external fields was conducted. Furthermore, the time-temperature-transformation curves (TTT curve) were obtained, and the microstructure and mechanical property of the alloy under the effect of different external fields were tested. Results indicated that the effect of magnetic field postponed the alloy's aging precipitation process, and slightly reduced its mechanical property; the effects of electric field accelerated the alloy's aging precipitation, increased its mechanical property and made the precipitated phase of alloy smaller and diffused. In addition, through analysis, it was concluded that the performance of the specimen was even more balanced under the effect of electromagnetic field.

Keywords: 2219 aluminum alloy; aging kinetics; diffusion activation energy; external fields

1. Introduction

It has been a permanent goal for material scientists to further increase and improve the structure and performance of materials. In recent years, quite a few researchers have applied external fields (electric field or magnetic field, etc.) into the solid-state phase transformation process of materials, and achieved certain results, which become a new method to improve material structure and performance. Shimotomai et al. [1] discovered that the magnetic field of 1.2 Tesla (T) was capable of significantly increasing the quantity of ferrites transformed from austenite in high-carbon steel; Yang et al. [2] studied the heat transfer in heat treatment process in a high-intensity magnetic field, and pointed out that high-intensity magnetic field could significantly accelerate heat transmission by conductivity in steel and facilitate a uniform cooling of steel, and magnetic field could provide phase transformation with a driving force; Wang et al. [3,4] applied DC of low current density (35 A/cm^2) into the aging process of Cu-Cr-Zr alloy after it has gone through solid solution and cool deformation, and the study showed that DC played a significant accelerator in the precipitation; after the current density was lifted up to 100 A/cm^2, the result showed that DC not only shortened the aging time needed to reach the maximum hardness from 4 h to 3 h, but the maximum hardness also increased 9 HV; Zhan et al. [5] studied the influence of electric pulse aging on the structure and performance of 7075 aluminum alloy, and it has been discovered that electric pulse accelerated the process of aging precipitation, increased the alloy's hardness, generating more precipitated phases from the alloy crystal and a higher degree of dispersion. All experiments mentioned above showed that external fields may bring about great influences on the structure of metals and alloys, thus enhancing their performance. Therefore, heat treatment under the effect of different external fields boasts a broad prospect of application. Current studies, however, are mainly focused on how external field parameters affect material performance and structure, yet few are concerned with the aging kinetics of aluminum alloy under the effect of external fields.

As a kind of Al-Cu-Mn aluminum alloy developed by ALCOA in the mid-20th century, 2219 aluminum alloy is of excellent thermal resistance, corrosion resistance and welding performance; hence it is widely used in the manufacturing of aerospace equipment, especially rocket fuel tank [6–8]. Researchers have conducted a lot of studies on 2219 aluminum alloy. Yang et al. [9] studied the influences of predeformation on the resilience, microscopic structures and mechanical properties of creep aging forming 2219 aluminum alloy, pointing out that predeformation could reduce resilience and improve the mechanical properties of the alloy. Chen et al. [10] studied the influences of different aging states on the friction stir welding of 2219 aluminum alloy plate, and found out that the strength coefficient of O-style plate was much higher than that of T6 alloy plate. Mazurina et al. [11], with channel angular pressing method, studied the influences of the deformation temperature from 250 to 475 °C on the changes of 2219 aluminum alloy's microscopic structures.

However, the studies on 2219 aluminum alloy at present are mainly focused on the aspects of mechanical property and material forming, while the studies on the aging kinetic behaviors of 2219 aluminum alloy under the effect of external fields are still rare. In view of that, this paper conducted aging treatments on 2219 aluminum alloy under the effect of different external fields, and studied the alloy's aging kinetic behaviors under the effect of different external fields with self-developed electric pulse facilities and magnetic field generators, in the hope to offer theoretical foundation for the improvement of 2219 aluminum alloy's performance and the planning of heat treatment techniques.

2. Materials and Methods

The experiment material, 2 mm thick O-style 2219 aluminum alloy plates, was provided by Southwest Aluminum (Group) Co., Ltd., Chongqing, China, see Table 1 for its chemical composition. The specimen was produced as illustrated in Figure 1. The specimen went through solid solution first, of which the conditions were 535 °C and 35 min, and then it was quickly quenched by the water of indoor temperature before aging treatment. In the experiment, the facility used in the magnetic field was a self-developed coil-wound AC magnetic field transmission facility, the working frequency of which is 50 Hz, and the average effective magnetic intensity is 0.1 T, which was applied in a vertical position of the specimen surface. The device used in electric field aging was a self-developed high-precision impulsive current generator , the electric pulse parameters of which are current density 80 A/cm^2, duty cycle D = 50%, pulse frequency f = 500 Hz, which was introduced from both ends of the specimen. The external field generator was turned on when the temperature of the aging furnace has reached to the level of aging treatment where the specimens were already placed inside. The application time of all external fields (magnetic field, current and current + magnetic) was 4 h in average. Artificial aging took over when the application of external fields ended until the needed duration was met. The specimens were polished after the aging, and then their hardness test was conducted with Vicker's hardness tester where five points of each specimen was tested so as to obtain their average value. The facility used in the specimens' tensile property tests was DDL1000 electric universal tester (Changchun Research Institute for Machanical Science Co., Ltd., Changchun, China), the tensile speed of which was 2 mm/min. The TEM (Transmission electron microscope) structural observation of the alloy was conducted with JEOL-2010 transmission electron microscope (JEOL Ltd., Tokyo, Japan), with its accelerating voltage being 200 KV. The TEM specimens were polished and prepared through twin-jet electropolishing, with electrolyte temperature being −25 °C–−35 °C and the voltage 15 V.

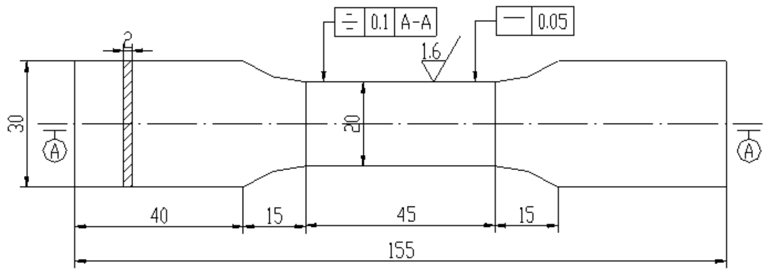

Figure 1. Tensile specimen size (unit: mm).

Table 1. Main chemical composition of 2219 aluminum alloy (mass fraction, %).

Cu	Mg	Mn	Si	Fe	Ni	Zr	Ti	Al
5.24	0.028	0.27	0.024	0.13	0.03	0.14	0.065	Bal.

3. Results and Discussion

3.1. Effects of Different External Fields on the 2219 Aging Process

Figure 2 showed the hardness curve under normal artificial aging and the application of different external fields in different aging temperatures (165 °C, 175 °C and 185 °C). Figure 2 indicated that the hardness value of the material showed a quick increase and then increase slowly and reached to the peak, then declined under the effects of various external fields. Moreover, as temperature rose, the aging time for the hardness to reach to the peak gradually declined, which meant that rising temperature may accelerate the aging process.

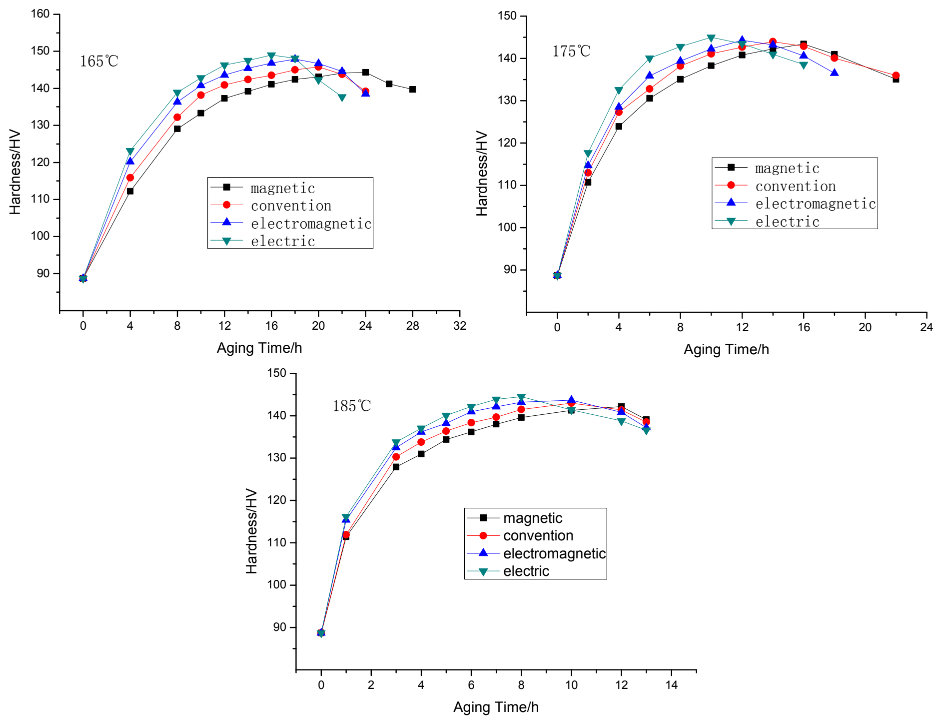

Figure 2. Ageing hardening curves under different external fields.

The time for the alloy's hardness to reach to its peak changed as external fields were introduced into the aging process, and the peak value changed as well. Under the condition of the aging temperature being 165 °C, it takes 20 h for conventional aging to reach to its peak, with the hardness being 145.8 HV; it takes 24 h for magnetic field aging, with the hardness being 144.3 HV, slightly smaller than that of conventional aging; while under the joint effect of current and magnetic fields (also known as electromagnetic field), it takes 18 h to reach to the peak, with the hardness being 147.9 HV, slightly higher than that of conventional aging; yet under the effect of current alone, it takes 16 h only for the alloy to reach peak, with the hardness being 149 HV, improving the performance of the alloy.

A curve is fitted with Avrami transformation kinetics [12], and the relation between the percentage of aging transformation f and the aging time t meet the following relation.

$$f = 1 - \exp(-kt^n) \tag{1}$$

where, f is percentage of aging transformation, t is ageing time, n is Avrami index, or hardening exponent, k is diffusion coefficient

$$k = k_0 \exp(-\frac{Q}{RT}) \tag{2}$$

where, k_0 is diffusion constant, R is gas constant, T is thermodynamic temperature, Q is diffusion activation energy. According to the analysis of the parameters in the formula, the main factors that affect diffusion are diffusion coefficient k_0, temperature T and diffusion activation energy Q etc. According to the performance of hardness in under-aged condition under the effect of different external fields, the percentage of aging transformation can be similarly expressed with the percentage f of aging hardness of different time lengths and peak hardness [12,13]

$$f = (H_t - H_0)/(H_{\max} - H_0) \tag{3}$$

In the formula, H_0 refers to the hardness in solid solution state, H_t is the hardness at the time t, and $H_{\max}$ is the peak hardness.

Since the hardness curve at the early aging stage can represent the aging precipitation kinetic equation, the over-aged hardness values under the effect of different external fields are fitted, and the fitting results are shown in Figure 3.

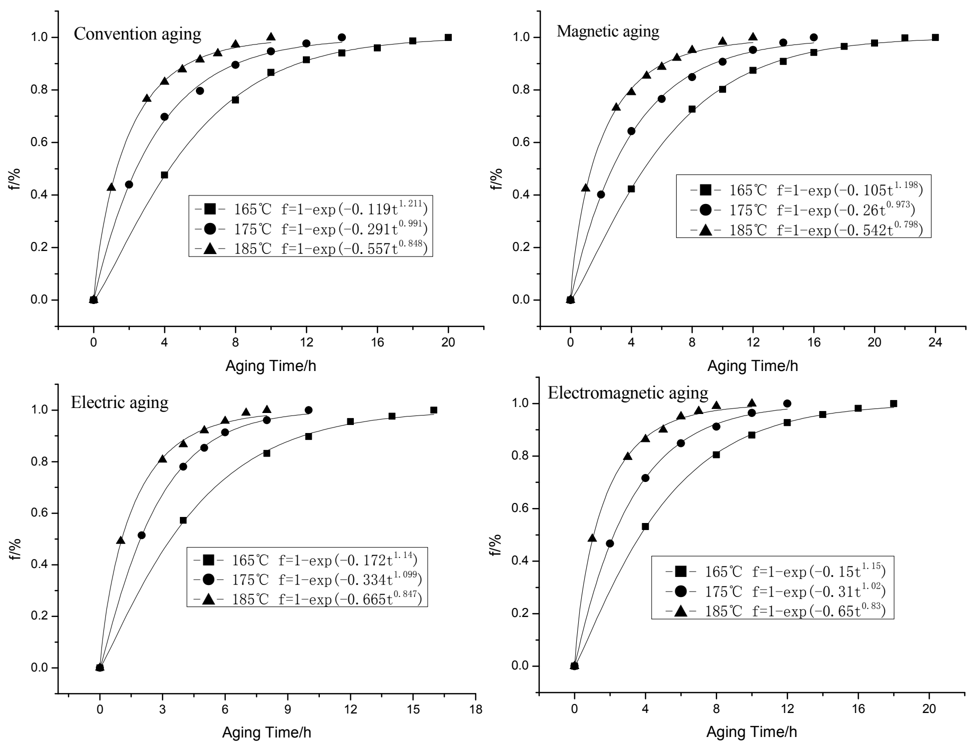

Figure 3. Fitting of aging kinetics curves.

Take the logarithms from both ends of Formula (2), and the formula after conversion $\ln k = \ln k_0 - Q/RT$ can be obtained. Take $1/RT$ as the abscissa, $\ln k$ as the ordinate, then they can be seen as a linear equation. With $-Q$ being seen as the slope and $\ln k_0$ as the intercept, the activation energy Q after conventional aging can be obtained through the linear fitting of $1/RT$ and $\ln k$ with the use of origin. The conventional aging fitting curve is shown in the following graph. Similarly, the curves under effect of other external fields can be fitted.

Figure 4 is a diagram of the relationship between Ink and $1/RT$ under the effects of normal conditions. The aging activation energies under the effects of normal conditions, magnetic field, current and electromagnetic field are 128.6 kJ/mol, 136.9 kJ/mol, 113.1 kJ/mol and 120.7 kJ/mol respectively. Compared with conventional aging, the effect of current and electromagnetic fields reduced the aging precipitation activation energy, while the effect of a single magnetic field increased the diffusion activation energy Q, indicating that current aging is easier to precipitate the second strengthening phase and more helpful to enhance the intensity of materials.

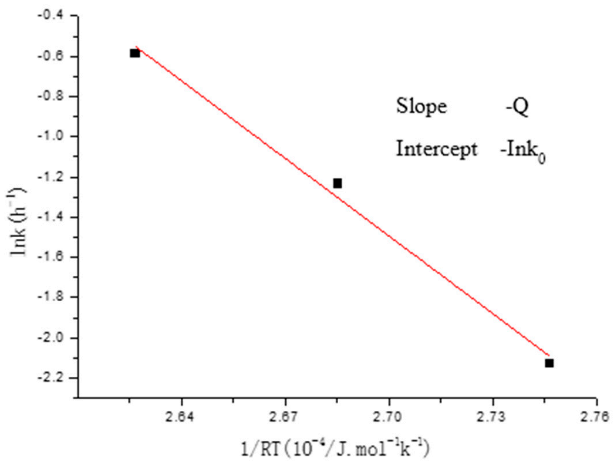

Figure 4. Relationship between Ink and $1/RT$.

3.2. TTT Curve under the Effects of Different External Fields

The completion of the materials' new phase precipitation of 10% and 95% are respectively set as the beginning time and finishing time of the transformation, i.e., substituting $f = 0.1$, $f = 0.95$ and the parameters of n and k in transformation kinetic formula in different states into Formula (4) to calculate the duration for beginning and finishing of precipitated phase transformation, with $\ln t$ seen as the horizontal axis, and the temperature as the vertical axis.

$$f = \exp\left\{\frac{1}{n}\ln(-\frac{\ln(1-f)}{k})\right\} \tag{4}$$

Therefore, the "C" curve of 2219 aluminum alloy time-temperature-transformation drawn is shown in Figure 5. It is observed that the time of transformation gradually shortens as temperature rises within the range of 165 °C–185 °C without any tip point. The departure line of phase transformation moves differently under the effect of different external fields; the time temperature transformation curve moves right under the effect of magnetic field in comparison with conventional aging, indicating that the application of magnetic field expands the induction period of aging process, and increases the completion time of phase transformation. However, the time temperature transformation curve moves left under the effect of electromagnetic field or current, indicating that the induction period of aging process is shortened. By comparison, it is discovered that the curve moves a slightly more left when it is under the effect of current, indicating that the induction period of phase transformation is the shortest under the effect of current, and so is the final completion time of phase transformation.

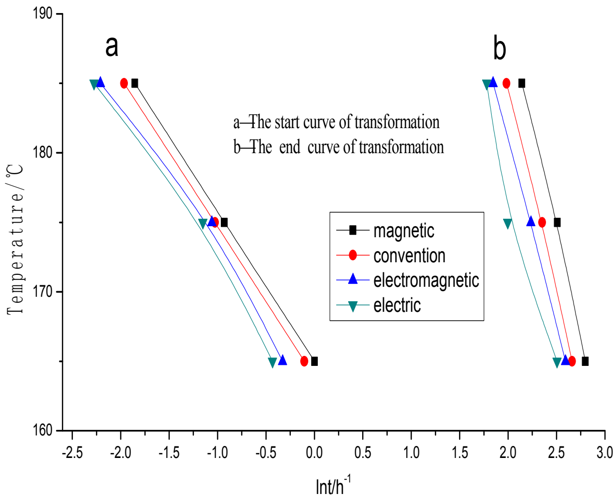

Figure 5. The time-temperature-transformation curves.

3.3. Effects of Different External Fields on the Microstructure

2219 aluminum alloy is a kind of alloy can be strengthened through heat treatment, the strengthening phase in the aging process is θ″ and θ′ phase and its the aging precipitation sequence is SSS-GP zone -θ″-θ′-θ [14]. Figure 6 shows the transgranular TEM microscopic structure of 2219 aluminum alloy which experienced the aging under the effect of different external fields for 4 h and then aging for additional 4 h at the temperature of 175 °C. It can be seen from Figure 7 that all transgranular precipitated phases are all mutually perpendicular needle-like phases whether under conventional aging or aging of external fields, indicating that the effects of external fields are incapable of changing the type of alloy precipitated phases. The quantity of transgranular precipitated phases reduced significantly without any obvious change in sizes under the effect of magnetic field; while the quantity of transgranular precipitated phases under current aging or electromagnetic field aging is higher than that of conventional aging, and the precipitated phases are smaller and diffused.

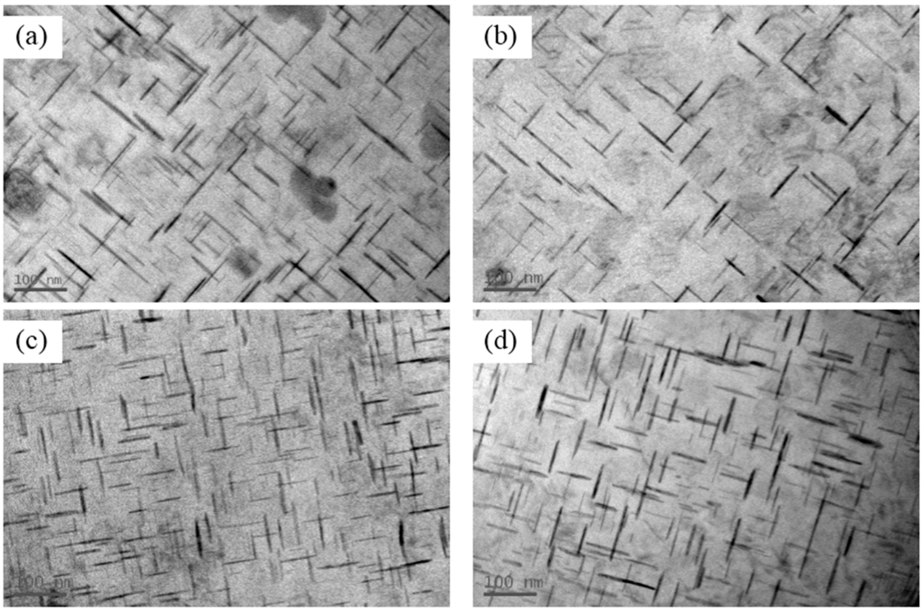

Figure 6. TEM images of 2219 aluminum alloy at 175 °C. (**a**) convention; (**b**) magnetic; (**c**) electric; (**d**) electromagnetic.

The aging of alloys is a process of solid-state phase transformation, the precipitation of second-phase particles, including their nucleation and growth. The nucleation rate of a homogeneous nucleation can be expressed as [15]

$$\dot{N} = K\exp\left(\frac{-\Delta G_k}{kT}\right)\exp\left(\frac{-\Delta G_A}{kT}\right) \tag{5}$$

where N is number of atoms in the parent phase of the unit volume, v is atomic vibration frequency; ΔG_k is nucleation work, ΔG_k is diffusion activation energy (Q), k is Boltzmann's constant; T is thermodynamic temperature.

It is known from the analysis above that magnetic field aging magnifies the diffusion activation energy of 2219 aluminum alloy and decreases its nucleation rate; while electric field aging and electromagnetic field aging decreases the diffusion activation energy of 2219 aluminum alloy and increases its nucleation rate. As a result, the quantity of precipitated phases of the alloy under magnetic field aging tends to be fewer than that under conventional aging, while the quantity of precipitated phases of the alloy under current aging and electromagnetic field aging tends to be more than that under conventional aging. Meanwhile, the sizes of transgranular phases under electric field aging and electromagnetic field aging tend to be smaller than that of conventional aging since electric field accelerates the nucleation rate of the alloy, leading to more and more diffused nucleation areas of precipitated phases, yet the number of vacancies inside the alloy reduces, and electric field aging accelerates the movement of vacancies, thus reducing the growth rate of second phase. The existence of electric field leads to the increase of the second phase's nucleation rate and the reduction of its growth rate, making it smaller in size yet higher degree of dispersion.

The current density of specimens appears to be higher due to the shortest way effect of current when under a single electric field aging, leading to unbalanced performances of specimens. If magnetic field is applied additionally, a Lorentz force will be generated upon the electrons of the alloy, thus leading to changes in the conditions of electron flow as shown in Figure 7.

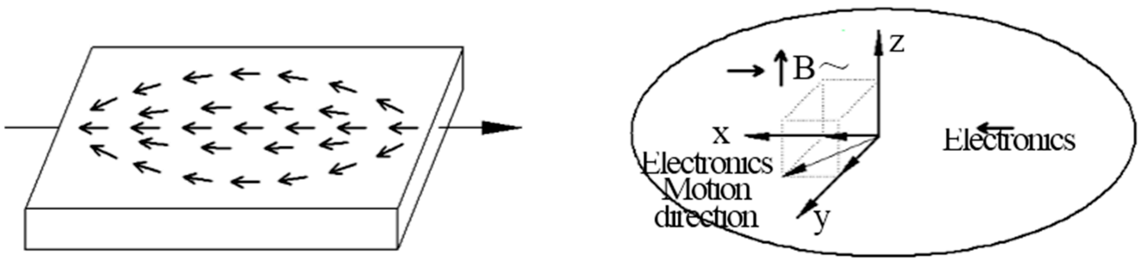

Figure 7. Schematic diagram of magnetic field on electron.

The application of magnetic field makes electrons flowing along the current bound by the Lorentz force. The current flows along the positive direction of x axis, and the magnetic field moves along the negative direction of z axis. It is known that the Lorentz force is applied upon electrons along the negative direction of y axis based on the left-hand rule, of which the intensity is shown in Formula (6).

$$F_{ev} = Bqv \tag{6}$$

In the formula, F_{ev} refers to the Lorentz force applied, B refers to the magnetic induction intensity, q is the charge of electrons, v refers to the velocity of electrons. Based on the analysis of Formula (5), it is known that as B changes with time, a Lorentz force along the positive/negative directions of y axis will be generated upon the electrons, homogenizing the strengthening effect of current on the alloy and improving the shortest way effect of the current, so that the alloy on the edges of materials can be strengthened as well, which will greatly homogenize the whole performance of the materials.

3.4. Effects of Different External Fields on the Mechanical Property

Table 2 indicates the mechanical property of the alloy after 8 h of conventional aging and the aging under the effect of different external fields with aging temperature being 175 °C. It is also known from Table 2 that the effects of different external fields all have impact on the mechanical property of the alloy. The intensity of the alloy is often slightly lower after magnetic field aging when compared with that after conventional aging; the alloy mechanical property peaks after current aging with the tensile strength reaching up to 387.22 Mpa, while the alloy's mechanical property is higher after electromagnetic field aging than that after conventional aging, and the intensity is not reduced when compared with that after current aging, indicating that the type of external fields and the duration of the effects have significant impact on the alloy's mechanical property; the existence of magnetic field reduces the mechanical property of materials, whereas the existence of electric field and electromagnetic field increases the mechanical property of materials.

Table 2. Effect of different external fields on the mechanical properties of the alloy.

Temperature/°C	External Field	Tensile Strength/MPa	Yield Strength/MPa	Elongation/%
175 °C	Convention	376.9	262.41	18.37
	Magnetic	375.81	257.38	16.05
	Electric	387.22	274.52	15.48
	Electromagnetic	387.5	270.35	15.2

The intensity of aluminum alloy is closely related to its microscopic structure, and the volume fraction of second phase particles and the degree of diffusion of precipitated phase particles have larger impact on the alloy mechanical property. Normally speaking, the bigger the volume fraction of precipitated phase is, the higher of the degree of diffusion will be, and the higher of the material intensity will be as well. The internal volume fraction of the alloy after magnetic aging is significantly reduced than that after conventional aging, hence its lower performance, whereas for the alloy after electric field aging and electromagnetic field aging, its volume fraction of precipitated phase is higher than that after conventional aging with higher degree of diffusion despite of its smaller internal precipitated phase, hence higher alloy intensity.

4. Conclusions

(1) The introduction of external fields changes the aging precipitation process of 2219 aluminum alloy, extending the time for the alloy to reach peak aging, whereas the application of electric field and electromagnetic field brings the peak aging time forward and increases the peak hardness of the alloy.

(2) Avrami empirical equation perfectly describes the aging kinetic behaviors of 2219 aluminum alloy, from which it can be known that the diffusion activation energy Q of current, electric field + magnetic field, conventional aging, and magnetic field gradually increases.

(3) During the aging process, the introduction of electric field magnifies the volume fraction, reduces the size, and increases the degree of diffusion of internal alloy precipitated phase; the introduction of magnetic field reduces the volume fraction of internal alloy precipitated phase; while the introduction of both electric field and magnetic field can not only guarantee that the mechanical property of the alloy does not decrease, but also make sure the stability of alloy performance.

Acknowledgments: This work was supported by the Fundamental Research Funds for the Central Universities of Central South University (No. 2016zzts318), the Key Program of the National Science Foundation of China (No. 51235010) and the National Key Basic Research Development Pan Funded Project of China (No. 2014cb046602).

Author Contributions: Wenke Li and Lihua Zhan conceived and designed the experiment; Qiangqiang Ma and Wenke Li performed the experiments; Wenke Li and Qiangqiang Ma analyzed the data; Lingfeng Liu contributed reagents, materials and analysis tools; Wenke Li wrote the paper.

Conflicts of Interest: The authors declare no conflict of interest.

References

1. Shimotomai, M.; Maruta, K.; Mine, K.; Matsui, M. Formation of aligned two-phase microstructures by applying a magnetic field during the austenite to ferrite transformation in steels. *Acta Mater.* **2003**, *51*, 2921–2932. [CrossRef]
2. Yang, G.; Feng, G.H. Phenomenon of heat conduction in the magnetic field heat treatment for ferritie and pearlitie steels. *J. Steel Iron Res.* **2000**, *12*, 31–35.
3. Wang, Z.; Zhong, Y.; Cao, G.; Wang, C.; Wang, J.; Ren, W.; Lei, Z.; Ren, Z. Influence of dc electric current on the hardness of thermally aged Cu-Cr-Zr alloy. *J. Alloys Compd.* **2009**, *479*, 303–306. [CrossRef]
4. Wang, Z.-Q.; Zhong, Y.-B.; Rao, X.-J.; Wang, C.; Wang, J.; Zhang, Z.-G.; Ren, W.-L.; Ren, Z.-M. Electrical and mechanical properties of Cu-Cr-Zr alloy aged under imposed direct continuous current. *Trans. Nonferrous Metals Soc. China* **2012**, *22*, 1106–1111. [CrossRef]
5. Zhan, L.; Jia, S.; Zhang, J. Influence of electrical impulse aging on microstructure and mechanical properties of 7075 aluminum alloy. *Trans. Nonferrous Metals Soc. China* **2014**, *3*, 600–605.
6. Wang, H.; Yi, Y.; Huang, S. Influence of pre-deformation and subsequent ageing on the hardening behavior and microstructure of 2219 aluminum alloy forgings. *J. Alloys Compd.* **2016**, *685*, 941–948. [CrossRef]
7. Owolabi, G.M.; Bolling, D.T.; Tiamiyu, A.A.; Abu, R.; Odeshi, A.G.; Whitworth, H.A. Shear strain localization in AA 2219-T8 aluminum alloy at high strain rates. *Mater. Sci. Eng. A* **2016**, *655*, 212–220. [CrossRef]
8. Li, Q.; Wu, A.; Li, Y.; Wang, G.; Yan, D.; Liu, J. Influence of temperature cycles on the microstructures and mechanical properties of the partially melted zone in the fusion welded joints of 2219 aluminum alloy. *Mater. Sci. Eng. A* **2015**, *623*, 38–48. [CrossRef]
9. Yang, Y.; Zhan, L.; Ma, Q.; Feng, J.; Li, X. Effect of pre-deformation on creep age forming of AA2219 plate: Springback, microstructures and mechanical properties. *J. Mater. Process. Technol.* **2016**, *229*, 697–702. [CrossRef]
10. Chen, Y.; Liu, H.; Feng, J. Friction stir welding characteristics of different heat-treated-state 2219 aluminum alloy plates. *Mater. Sci. Eng. A* **2006**, *420*, 21–25. [CrossRef]
11. Mazurina, I.; Sakai, T.; Miura, H.; Sitdikov, O.; Kaibyshev, R. Effect of deformation temperature on microstructure evolution in aluminum alloy 2219 during hot ECAP. *Mater. Sci. Eng. A* **2008**, *486*, 662–671. [CrossRef]
12. Li, Y.; Yi, D. Dynamics of phase transfomation in Cu-Fe-Ag alloy. *Trans. Metal Heat Treat.* **2010**, *5*, 49–52.
13. Zhang, J.; Zhan, L.; Jia, S. Effects of Electric Pulse Current on the Aging Kinetics of 2219 Aluminum Alloy. *Adv. Mater. Sci. Eng.* **2014**, *2014*, 1–8. [CrossRef]
14. Ber, L.B. Accelerated artificial ageing regimes of commercial aluminium alloys. II: Al-Cu, Al-Zn-Mg-(Cu), Al-Mg-Si-(Cu) alloys. *Mater. Sci. Eng. A* **2000**, *280*, 91–96. [CrossRef]
15. Zheng, Z. *Fundamentals of Material Science*, 1st ed.; Science Press: Beijing, China, 2007.